The effect of titanium dioxide nanoparticles with or without platelet rich plasma on the healing of mandibular bony defects in rabbits

Maha H. Ibrahim[a], Omaima H. Afifi[a], Shoukria M. Ghoneim[b], Doaa A. Youssef[a]

[a]Department of Oral Medicine, Periodontology, Oral Diagnosis and Oral Radiology, Faculty of Dentistry, Tanta University, Egypt, [b]Department of Oral Pathology, Faculty of Dentistry, Tanta University, Egypt

Correspondence to Maha H. Ibrahim, MSc, Assistant Lecturer of Oral Medicine, Periodontology, Oral Diagnosis and Oral Radiology, Faculty of Dentistry, Tanta University, Egypt,
Postal/zip code: 32951;
Fax numbers: 3335631;
Tel number: 01069077416.
E-mail: maha.hasan2003.mh@gmail.com

Received 25 November 2021
Revised 08 January 2022
Accepted 09 January 2022
Published 10 June 2022

Tanta Dental Journal
2022, 19:68–76

Objectives
This experimental study was designed to evaluate the effect of titanium dioxide nanoparticles (TiO_2NPs) alone or in combination with platelet rich plasma (PRP) on the healing of experimentally created critical-size bony defects in the rabbit's mandible histologically, immunohistochemically using matrix metalloproteinase-9 and vascular endothelial growth factor antibodies and histomorphometrically.

Materials and methods
Sixteen rabbits were included in the study, where three identical critical-size circular bony defects, two in the right side and one in the left side of the mandible of each rabbit, were created; group I: comprises 16 intraosseous defects (the mesial defect in the right side of the mandible of each rabbit) with no filler, group II: comprises 16 intraosseous defects (the distal defect in the right side of the mandible of each rabbit) filled with TiO_2NPs powder mixed with saline, group III: comprises 16 intraosseous defects (the defect in the left side of the mandible of each rabbit) filled with TiO_2NPs powder mixed with PRP. Samples were collected from the surgical sites of the experimental defects at 2 and 6 weeks.

Results
Histologically and histomorphometrically: the amount of newly formed bone was superior and significant in group III when compared with group II and group I at 2 and 6 weeks interval. Immunohistochemically group III showed superior and statistically significant increase in the vascular endothelial growth factor expression levels and matrix metalloproteinase-9 immunolabeling when compared with group II and group I.

Conclusion
TiO_2NPs can be considered a promising material for bone regeneration alone or when combined with PRP.

Keywords:
critical-size bony defects, metalloproteinase, platelet rich plasma, titanium dioxide nanoparticles, vascular endothelial growth factor

Tanta Dental Journal 19:68–76

1687-8574

Introduction

The most positive outcome of periodontal regeneration procedures in intrabony defects has been achieved with bone grafts, root bio-modifications, application of growth factors, guided tissue regeneration, and combination of these procedures [1].

A number of natural and synthetic bone graft alternatives have been utilized for periodontal regeneration [2]. Synthetic bone graft substitutes provide both biocompatible environment and immediate physical support that support osteogenesis, enhance vascularization and bio-mineralization [2,3].

Nanostructured titanium dioxide (TiO_2) was designed and manufactured as a synthetic ceramic bone graft substitute material because of their excellent qualities such as excellent biocompatibility, high tensile strength, high corrosion resistance, flexibility, low-cost, low solubility, high stability, low toxicity and safe toward both the environment and humans, therefore preferred in biological research and other applications [4,5].

Additionally, nano-TiO_2 is considered a promising osteoconductive bone graft material [6,7]. It showed high surface-to-volume ratio which is needed to reach sufficient cell attachment and growth for tissue regeneration [3]. Besides, It has been documented in many studies that it also obtains considerably high porosity, hence, improves the osteogenesis [3,8,9].

Interestingly, TiO_2 and its variants are novel antimicrobials that have the potential to combat

human pathogenic micro-organisms [10]. Titanium dioxide nanoparticles (TiO_2NPs) coated on prosthetic implants have been found to be utilized to reduce problems and infections after surgery because of their antibacterial activity [11].

Growth factors have been used to enhance bone and soft tissue repair, including blood autologous growth factors produced after platelet activation, for example platelet rich plasma (PRP), platelet rich fibrin and concentrated growth factor [12].

A concentrated suspension of many growth factors can be derived from autologous sources such as PRP. These factors include fibroblast growth factor (FGF), vascular endothelial growth factor (VEGF), platelet derived growth factor (PDGF), transforming growth factor (TGF), insulin like growth factor, bone morphogenic protein and epithelial growth factor [13,14]. They enhance cell replication (mitogenesis), regulate proliferation and differentiation of multiple cell types and stimulate the budding of new capillaries (angiogenesis) [15].

The angiogenesis is regulated by several growth factors like: VEGF, PDGF, epithelial growth factor, FGF, angiopoietin, TGF-β and tumor necrosis factor-alpha [16]. VEGF is considered the most essential factor in the regulation of angiogenesis [16,17].

Admittedly, osteogenesis and bone remodeling are matrix metalloproteinases (MMPs) dependent processes. The family of MMPs consists of more than 25 enzymes in four subfamilies which have pivotal function in extracellular matrix remodeling [18]. Gelatinases (MMP-2 and MMP-9) subfamily are differentially expressed by osteogenic and connective tissue cells during several events of bone regeneration [18–20].

Accordingly, the present study was conducted to evaluate the effect of TiO_2NPs alone or in combination with PRP on the healing of experimentally created critical-size bony defects in the rabbit's mandible histologically, immunohistochemically using MMP-9 and VEGF antibodies and histomorphometrically.

Materials and methods

(1) TiO_2NPs (supplied as a powder form, with particle size 50 nm).
(2) PRP.
(3) Centrifuge device.
(4) A trephine bur.

A stainless-steel bur with a diameter 5 mm, a high-efficient toothed-like end and openings in its working area, used in a slow speed contra-angle hand piece.

Animal selection

Sixteen male adult rabbits were selected in this experimental study, about 3–6 months of age, weighing about 1.5–2 kg. Animals were held in separate cages and fed on standard food. In compliance with standards on the appropriate use of animals in research, the experiment protocol was established in accordance with scientific research ethics criteria of Research Ethics Committee, Faculty of Dentistry, Tanta University.

Platelet rich plasma preparation

Five milliliters blood was withdrawn from each animal through retro-orbital venous plexus using a capillary tube into a tube containing citrate phosphate dextrose solution as an anticoagulant. Then, the blood was centrifuged for 10 min at 1300 rpm (soft spin). The first step of centrifugation separated the whole blood into three fractions: an upper yellow fraction containing platelet poor plasma on top, a thin intermediate layer containing leukocytes and platelet (buffy coat) and the dense layer containing red blood cells at the bottom. The platelet poor plasma and the middle buffy coat layer were centrifuged for a second time for 10 min at 2000 rpm (hard spin) after being aspirated and transferred to another clean tube. This resulted in a lower red tinged layer of highly concentrated PRP and an upper portion of clear yellow supernatant serum [21].

Surgical procedure and postoperative care

General anesthesia obtained with intramuscular injection of a combination of ketamine hydrochloride 30 mg/kg body weight and Xylazine 5 mg/kg body weight. Using an extraoral approach, a shallow midline vertical incision was done along the inferior surface of the mandible from the chin to a line perpendicular to the gonial angles of the mandible. Then, a lateral reflection and blunt dissection was made [22]. Once the lateral aspect of the mandible exposed, a trephine bur with a diameter of 5 mm in a slow speed contra-angle hand piece 1000 rpm under constant external cooling with sterile physiological saline solution was used to create three identical circular critical-size bony defects.

All defects were made in the same way and grouped to be treated as follows:

(1) Group I (control group): comprises 16 intraosseous defect sites (the mesial defect in the right side of the mandible of each rabbit) with no filler.

(2) Group II (TiO_2NPs-treated group): comprises 16 intraosseous defect sites (the distal defect in the right side of the mandible of each rabbit) filled with TiO_2NPs powder mixed with saline with a ratio 2: 1.
(3) Group III (TiO_2NPs + PRP-treated group): comprises 16 intraosseous defect sites (the defect in the left side of the mandible of each rabbit) filled with TiO_2NPs powder mixed with PRP with a ratio 2:1.

Tissues were carefully repositioned and sutured in separate layers.

Postoperative care included administration of 0.1 ml of ketoprofen intramuscular daily for up to 3 consecutive days. In addition (cefotaxime sodium 0.5 gm) was administered intramuscular daily for up to 4 consecutive days. Sutures were removed 7 days postsurgery.

Euthanasia

Two weeks following the surgery, eight rabbits were euthanized while the remaining rabbits were euthanized 6 weeks postsurgery. This was performed using barbiturate anesthetic overdose of thiopental sodium (Thiopentax) intramuscular (3 ml). Mandibles of all euthanized rabbits were dissected carefully, all collected samples from the surgical areas of the experimental defects were handled for further immunohistochemical and histological analysis and histomorphometric examinations.

Tissue preparation

Tissue specimens were immediately preserved for at least 12 h in 10% neutral phosphate buffered formalin, then, in 10% EDTA solution containing 5% sodium sulfide, specimens were decalcified until demineralization occur. The bone specimens were dehydrated in ascending grades of alcohols (70, 90, 100%) for 2 h per each, then were fixed in paraffin wax. Mesio-distal serial sections of 5 μm were cut after the blocks were fixed on the microtome and installed on a positively charged glass slides. Harris' hematoxylin and eosin (H&E) was used to stain representative portions [23] following the routine technique for conventional histological assessment. The sections were examined under light microscope.

Immunohistochemical assessment

The avidin–biotin–peroxidase complex was used for immunohistochemical labeling method [24]. Xylene were used to deparaffinize representative sections acquired from the central part of the defects. The sections were rehydrated using a series of descending concentrations of ethanol then washed in buffer. Then, to inhibit endogenous peroxidase, they were incubated in hydrogen peroxide in dH_2O at room temperature for about 30 min. Antigen was retrieved as instructed by manufacture. Slides were immersed in 100 μl blocking solution (Abcam) at normal temperature for 30 min. Primary antibodies were applied overnight at 4°C in dilutions as recommended. Sections were washed in phosphate buffered saline prior to being incubated in a humidified chamber at ambient temperature for 1 h within secondary biotinylated antibody in blocking buffer (primary and secondary antibodies as well as other reagents used in this study are summarized in Table 1). Incubation of sections in avidin–biotin–peroxidase complex solution at normal temperature for 1 h was required for peroxidase visualization. Diaminobenzidine solution (0.5 mg/ml diaminobenzidine and 0.1% H_2O) was added onto the sections to emerge color reaction. Once the reaction was satisfying, it was ceased by wash out with H_2O for 5–10 min. After that, using Myer's hematoxylin for 2 min, sections were counterstained. Finally, sections were gradually dehydrated and mounted with coverslips. Light microscope was used for immunohistochemical staining assessment.

Histomorphometric assessment and semiquantitative analysis

ImageJ software (Public domain, image processing and analysis in Java, http://rsb.info.nih.gov/ij/) were used for image analysis to calculate the extent of new bone formation and measure the intensity of MMP-9 immunoreactivity. VEGF immunostaining was quantified using semiquantitative method as described by Klein *et al.* [25] with modification by calculation of the expression index that associate the area fraction of labeled cells with the immunostaining intensity obtained by visual qualitative observation.

Statistical analysis

Statistical presentation and analysis of the present study was conducted, using SPSS, version 21. Quantitative variables were expressed as mean and SD and paired *t* test were applied to compare between

Table 1 Antibodies and other reagents

Antibody	Source	Cat. no
Anti-MMP-9 primary antibody (Mouse monoclonal to MMP-9)	Abcam, UK	ab58803
Secondary to MMP-9 [goat anti-Mouse IgG H&L (HRP)]	Abcam, UK	ab205719
Anti-VEGF primary antibody (rabbit polyclonal to VEGF)	Abcam, UK	ab9570
Secondary to VEGF [goat anti-rabbit IgG HL (HRP)]	Abcam, UK	ab205718

MMP-9, matrix metalloproteinase-9; VEGF, vascular endothelial growth factor.

two studied dependent normally distributed variables. Comparisons were performed on more than two independent normally distributed subgroups using one-way analysis of variance test. Post-hoc multiple comparisons was done using Games-Howell.

Results

Histological and histomorphometrical results

At 2-week interval, H&E-stained sections of group I revealed highly vascular connective tissue was observed filling the bony defect while at 6 weeks interval, thin new bone formation that was insufficient to fill the entire defect was noticed (Fig. 1).

Regarding group II bone formation was represented by a thick layer of newly formed bone lining the entire wall of the defect surrounded by many osteoblast cells at 2 weeks interval. While, at 6 weeks evaluation period, well-organized newly formed trabecular bone was exhibited, and remnants of graft material within osteoid tissue were detected (Fig. 2).

H&E-stained sections of group III showed complete healing represented by a large quantity of thin and well-organized newly formed woven bone and osteoid tissue surrounded by active osteoblasts at 2 weeks interval. Thereafter, progressed to show complete osseous healing at 6 weeks (Fig. 3).

A histomorphometric analysis confirmed the histopathological results, which showed a statistically significant difference regarding the new bone formation percentage for group III in comparison to group II and group I at 2 and 6 weeks intervals (P = 0.000). Also, there were a statistically significant difference for group II by comparison to group I at both periods of evaluation (P = 0.000) at 2 weeks and (P = 0.004) at 6 weeks interval (Table 2).

Immunohistochemical and histomorphometrical results

Immunohistochemical findings of this study illustrated that, the three studied groups showed comparable superior results of angiogenesis mediated by an increase the intensity of VEGF expression levels at 2 weeks interval (Fig. 4). At 6 weeks interval, high intensity of VEGF expression levels was maintained regarding group III, while group I and group II showed decrease in the angiogenesis levels (Fig. 5).

The immunohistochemical findings were confirmed by semiquantitative analysis; there was a decrease in VEGF expression index values at 2 weeks among the groups that was not significant (P = 0.263). While at 6 weeks interval, group III had statistically significant increase in the VEGF expression index values when compared with group II and the control group (P = 0.008) (Table 3).

At 2 weeks interval, the three studied groups showed intense MMP-9 immunolabeling (Fig. 6). While at 6 weeks, group III showed marked and obvious MMP-9 immunolabeling than group II and both were more than group I (Fig. 7).

Figure 1

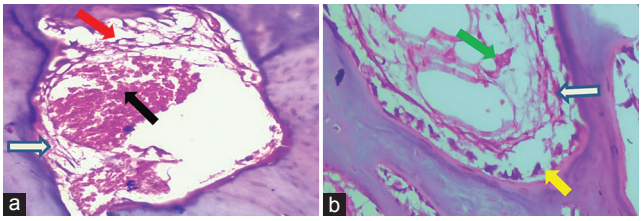

(a) Histological view of group I after 2 weeks showing granulation tissue consist of fibrous connective tissue (white arrow), numerous blood capillaries (red arrow), and heavy infiltration of chronic inflammatory cells (black arrow); (b) after 6 weeks showing thin layer of new bone surrounded by osteoblast cells (yellow arrow) and fibrous connective tissue (white arrow), and few areas of osteoid tissue (green arrow) (H&E, ×400). H and E, hematoxylin and eosin.

Figure 2

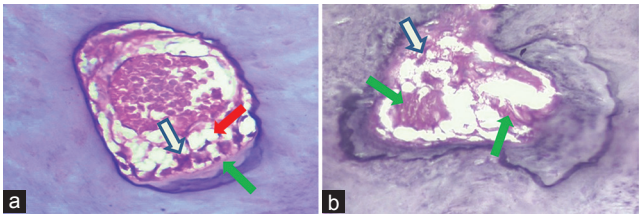

(a) Histological view of group II after 2 weeks showing remnant TiO_2NPs (white arrow) surrounded by numerous dilated blood capillaries (red arrow) and osteoid tissue (green arrow); (b) after 6 weeks showing thick newly formed trabecular bone and remnants of TiO_2NPs (white arrow) surrounded by osteoid tissues (green arrows) (H&E, ×400). H and E, hematoxylin and eosin; TiO_2NPs, titanium dioxide nanoparticles.

Figure 3

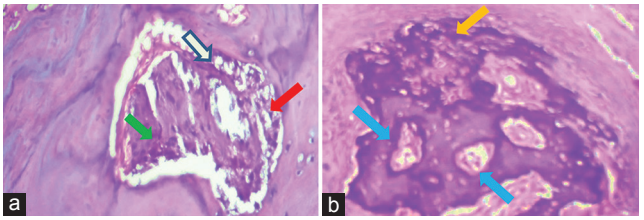

(a) Histological view of group III after 2 weeks showing remnant of TiO_2NPs (white arrow) surrounded by osteoid tissue (green arrow) and dilated blood capillaries (red arrow); (b) after 6 weeks showing remnant of woven bone (yellow arrow) and formation of cancellous bone (blue arrow) that completely fill the entire cavity. (H and E, ×400). H and E, hematoxylin and eosin; TiO_2NPs, titanium dioxide nanoparticles.

Table 2 Intragroup and intergroup comparison of the mean new formed bone percentage at 2 and 6 weeks interval

	Groups			ANOVA test
	GI (control) (*n*=8)	GII (TiO2NPs) (*n*=8)	GIII (TiO2NPs + PRP) (*n*=8)	
Newly formed bone (%) 2 weeks				
Mean±SD	0.30±0.29	1.71±0.44	3.38±0.63	*F*=85.601 *P*=0.000*
Pairwise comparison using Games-Howell test				
Control		Diff=−1.41600 *P*=0.000*	Diff=−3.08525 *P*=0.000*	
TiO_2NPs			Diff=−1.66925 *P*=0.000*	
TiO_2NPs + PRP				
Newly formed bone (%) 6 weeks				
Mean±SD	1.56±0.67	3.11±0.85	5.34±0.68	*F*=52.834 *P*=0.000*
Pairwise comparison using Games-Howell test				
Control		Diff=−1.54712 *P*=0.004*	Diff=−3.77763 *P*=0.000*	
TiO_2NPs			Diff=−2.23050 *P*=0.000*	
TiO_2NPs + PRP				
Paired samples test				
P	$t_{(DF=7)}$=4.498 *P*=0.003*	$t_{(DF=7)}$=5.376 *P*=0.001*	$t_{(DF=7)}$=10.596 *P*=0.000*	

*Statistically significant (*P*<o.o5) ANOVA, analysis of variance; DF, degree of freedom; PRP, platelet rich plasma; TiO_2NPs, titanium dioxide nanoparticles.

Table 3 Intragroup and intergroup comparison of the mean of vascular endothelial growth factor expression index values at 2 and 6 weeks interval

	Groups			ANOVA test
	GI (control) (*n*=8)	GII (TiO2NPs) (*n*=8)	GIII (TiO2NPs + PRP) (*n*=8)	
Expression index values 2 weeks				
Mean±SD	108.25±50.12	90.50±28.52	78.20±2.76	*F*=1.425 *P*=0.263 NS
Expression index values 6 weeks				
Mean±SD	33.93±17.63	33.88±14.16	88.00±35.52	*F*=13.207 *P*=0.000*
Pairwise comparison using Games-Howell test				
Control		Diff=−0.05000 *P*=1.000 NS	Diff=−54.07500 *P*=0.008*	
TiO_2NPs			Diff=−54.12500 *P*=0.008*	
TiO_2NPs + PRP				
Paired samples test				
P	*t* (DF=7)=4.901 *P*=0.002*	*t* (DF=7)=5.337 *P*=0.001*	*t* (DF=7)=0.854 *P*=0.421 NS	

*Statistically significant (*P*<o.o5), ANOVA, analysis of variance; DF, degree of freedom; PRP, platelet rich plasma; TiO_2NPs, titanium dioxide nanoparticles.

Figure 4

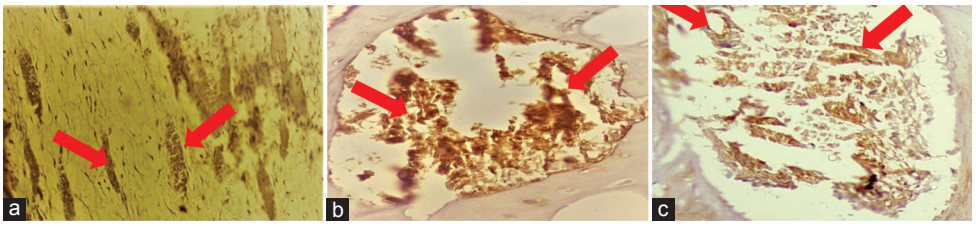

Histological views of the three studied groups stained with anti-VEGF after 2 weeks (a–c); (a) group I displaying positive stained endothelial cells lining the numerous dilated capillaries (red arrows). (b) Group II showing numerous stained dilated blood capillaries (red arrows) surrounding TiO_2NPs. (c) Group III showing numerous positive stained dilated blood capillaries (red arrows). (immunostain anti-VEGF, ×400). TiO_2NPs, titanium dioxide nanoparticles; VEGF, vascular endothelial growth factor.

It was observed by histomorphometrical analysis that, there was a statistically significant difference regarding the intensity of MMP-9 expression in favor of group III when compared with group I (P = 0.000) and no statistically significant difference when compared with group II at 2 weeks interval. While at 6 weeks, when group II and group III were compared to group I, there was a significant statistical difference in support of

Table 4 Intragroup and intergroup comparison of the mean intensity of matrix metalloproteinase-9 expression percentage at 2 and 6 weeks interval

	Group			ANOVA test
	GI (control) (*n*=8)	GII (TiO2NPs) (*n*=8)	GIII (TiO2NPs + PRP) (*n*=8)	
Intensity of MMP-9 expression (%) 2 weeks				
Mean±SD	1.48±0.89	2.90±1.45	3.89±0.50	*F*=11.225 *P*=0.000*
Pairwise comparison using Games-Howell test				
Control		Diff=−1.41696 *P*=0.087 NS	Diff=−2.41230 *P*=0.000*	
TiO_2NPs			Diff=−0.99534 *P*=0.214 NS	
TiO_2NPs + PRP				
Intensity of MMP-9 expression (%) 6 weeks				
Mean±SD	2.19±0.46	3.66±0.52	4.69±1.37	*F*=15.973 *P*=0.000*
Pairwise comparison using Games-Howell test				
Control		Diff=−1.47518 *P*=0.000*	Diff=−2.49785 *P*=0.003*	
TiO_2NPs			Diff=−1.02268 *P*=0.175 NS	
TiO_2NPs + PRP				
Paired samples test				
P	*t* (DF=7)=1.618 *P*=0.150 NS	*t* (DF=7)=1.665 *P*=0.140 NS	*t* (DF=7)=1.586 *P*=0.157 NS	

ANOVA, analysis of variance; DF, degree of freedom; MMP-9, matrix metalloproteinase-9; PRP, platelet rich plasma; TiO_2NPs, titanium dioxide nanoparticles; NS, statistically not significant (*P*>0.05).
*Statistically significant (*P*<0.05).

Figure 5

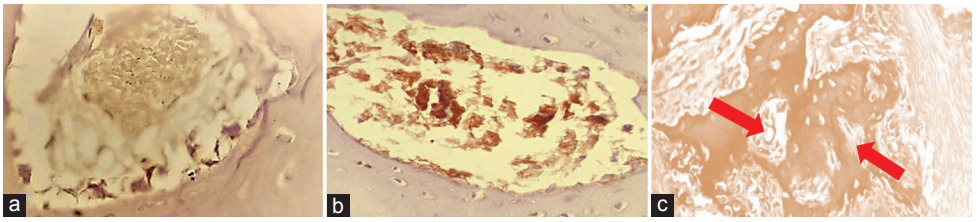

Histological views of the three studied groups stained with anti-VEGF after 6 weeks (a–c); (a) group I displaying decrease in stained dilated blood capillaries. (b) Group II showing lesser number of stained dilated blood capillaries surrounding TiO_2NPs (c) Group III showing intense positive reaction for anti-VEGF in the dilated blood capillaries present in marrow spaces (red arrows). (immunostain anti-VEGF, ×400). TiO_2NPs, titanium dioxide nanoparticles; VEGF, vascular endothelial growth factor.

Figure 6

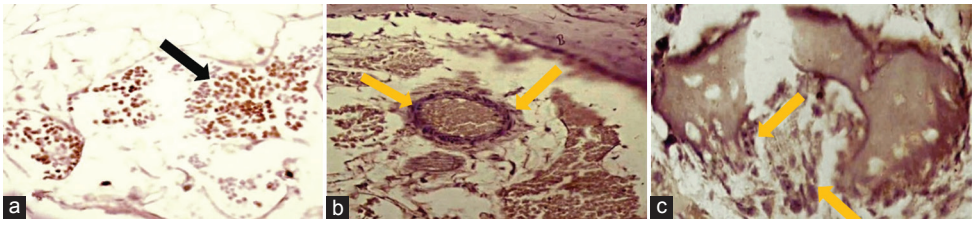

Histological views of the three studied groups stained with anti-MMP-9 after 2 weeks (a–c); (a) group I displaying intense positive reaction to anti-MMP-9 within the heavy infiltrated inflammatory cells (black arrow) of the granulation tissue. (b) Group II displaying intense positive staining for anti-MMP-9 in osteoblasts (yellow arrows). (c) Group III exhibit numerous osteoblast cells stained positive with anti-MMP-9 (yellow arrows) (immunostain anti-MMP-9, ×400). MMP-9, matrix metalloproteinase-9.

group II and group III with no statistically significant difference between both groups (Table 4).

Discussion

The scope of periodontal tissue engineering is to regenerate the tooth supporting tissues through a combination of proper biomaterials, which stimulate progenitor cells to produce new healthy tissues [26]. Development of an ideal graft substitute material has remained elusive due to the highly dynamic and nanoscale nature of bone.

To overcome this challenge, nanosized ceramics have been developed as a promising class of alloplastic

Figure 7

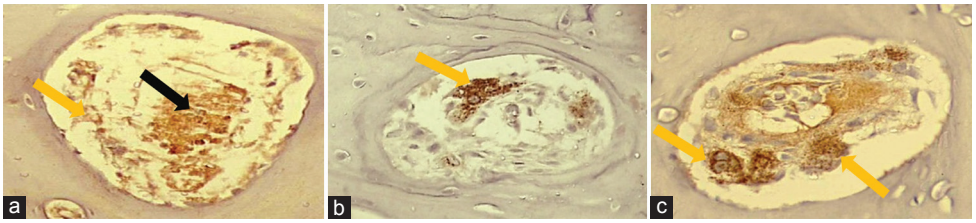

Histological views of the three studied groups stained with anti-MMP-9 after 6 weeks (a–c); (a) group I exhibit moderate positive reaction to anti-MMP-9 not only within the chronic inflammatory cells (black arrow) in the entire cavity but also within the few osteoblast cells (yellow arrow) lining the entire wall of the cavity. (b) Group II displaying an intense positive stained osteoblast cells (yellow arrow) with anti-MMP-9 within an area of osteoid tissue. (c) Group III exhibit intense positive reaction to anti-MMP-9 in osteoblast cells (yellow arrows) (immunostain anti-MMP-9, ×400). MMP-9, matrix metalloproteinase-9.

bone graft substitutes due to their improved osseo-regenerative performance [27]. Among the synthetic ceramic bone grafting materials TiO_2NPs has emerged as a promising candidate for bone regeneration [28]. PRP was selected in the current study as it has proven to promote graft vascularization, stimulates soft tissue healing, improve handling of particulate graft material and easier packing into the grafting site, thus facilitating space maintenance and potentiating bone regeneration [29,30]. Moreover, it provides essential growth factors and cytokines to the injured site by functioning as a biomaterial for enhancing rapid regeneration [31]. In the current study, histological and immunohistochemical analysis using VEGF and MMP-9 antibodies were assessed to clarify the effect of TiO_2NPs alone or in combination with PRP on the healing of experimentally created critical-size bony defects in the rabbit's mandible.

The outstanding results in group III revealed that the synergistic and combined effect of PRP with TiO_2NPs significantly enhanced and maintained the improvement of bone healing which might be attributed to the fundamental role of PRP in the early formation of a homogenous initial blood coagulum and its development into a provisional matrix thorough the bony defect [32].

In addition, it could be also attributed to the interesting biological means of PRP in the tissue repair through release of various growth factors such as TGF-β, VEGF, PDGF, and FGF [33,34] that are multifunctional cytokines and key regulators of bone development [35,36]. In line with this, Marx *et al.* [37], proposed that the addition of PRP to bone grafts enhanced bone formation degree and rate.

Furthermore, it may also be explained by the combined osteoconductive effect of nano-TiO_2 material with the biological synergistic effect of PRP as it was reported by several studies that the type of biomaterial combined with PRP might strongly influence its efficacy for bone regeneration [38–41].

The significant improvement in the mean percentage of new formed bone in group II and group III at both evaluation periods could be speculated that the direct stimulatory effect of TiO_2NPs on osteoblast cell functions (differentiation, adhesion, synthesis of alkaline phosphatase that is one of the important marker essential for osteogenesis) had a profound role in the significant improvement of bone healing [42,43]. In addition, it was reported that TiO_2NPs have a motivating action on the osteoblasts to produce bone morphogenic protein, which are known to initiate and regulate bone formation starting from the progenitor cell [43,44]. Furthermore, the porous architecture of TiO_2NPs provided an efficient substrate for proliferation of mesenchymal stem cells (MSCs) favoring osteogenesis [3,45,46].

In the current study, when the defect was left to heal spontaneously in group I (control group), highly vascular connective tissue was observed filling the bony defect at 2 weeks interval. While new bone formation was thin and insufficient to fill the entire defect at 6 weeks interval. This observation supported the findings reported by several authors concerned with the nonspontaneous and incomplete osseous healing of critical-size defects in rabbit mandibles over a long period of time [47–50].

Immunohistochemical findings of this study illustrated that, there was increase in VEGF expression levels surrounding TiO_2NPs at 2 and 6 weeks interval in group III that might be contributed to the significant effect of PRP which increase the number of matured blood vessels. This occur through angiogenic growth factors including VEGF and PDGF which accelerate angiogenesis during the early phase of healing, hence, maintain long-term improvement in osteogenesis [51]. These results were confirmed by Kim *et al.* [52], who reported that the angiogenic potential of PRP can be advantageous when grafted with noncellular alloplastic graft material leading to faster and more extensive new bone formation in the critical size bone defect.

The maintained increase in VEGF expression levels observed in group III could also be estimated by the profound effect of TiO_2NPs when mixed with PRP as it produced a cohesive mass, which improved the retention and slow release of many potent angiogenic growth factors because of slow degradation rate of the nanoparticles and thereby effectively restored revascularization. This phenomena was in line with Bir *et al.* [53], who found that incorporation PRP with gelatin hydrogel acted as a slow and sustained release carrier for growth factors in diabetic rats.

Regarding group I and group II, several mechanisms may explain the significant decrease in VEGF expression levels from 2 to 6 weeks. Angiogenesis is known to occur as soon as tissue damage occurs, and it remains active over the process of wound healing until it is finally suppressed at the terminal stages of healing as tissue hypoxia is restored which might be a contributing mechanism for this phenomena [54]. Other explanations might be regarded to the subside of inflammation and the decline in the levels of growth factors by the end of the healing process [55].

These results were in context with Boëck-Neto *et al.* [56], and Di Stefano *et al.* [57], who reported a high intensity of VEGF expression in the newly formed bone, while a low intensity was found in the mature bone.

The interesting results showed in group III regarding the increase in MMP-9 expression levels may strongly related to the reliable initiator role of PRP in the healing process. This occurs through release of three proteins from platelets that known to act as cell adhesion molecules: fibrin, fibronectin, and vitronectin which have sticky characteristic and act as a substrate for bone matrix formation [58,59]. Additionally, various growth factors released from PRP produce a multitude of effects on both fibroblast and osteoblast cells [60]. These findings were in harmony with Shin and Oh [61], who reported the effective role of PRP on the regulation of extracellular matrix remodeling and acceleration of wound healing events in wounds of diabetic rats.

The comparable favorable results of group II and group III regarding the increase in MMP-9 immunolabeling may be attributed to the direct stimulatory effects of TiO_2NPs on bone cells functions such as differentiation, adhesion, proliferation and expression of MMPs by osteogenic and connective tissue cells during several events of bone regeneration including MMP-9 that is considered to play an important role in extracellular matrix remodeling [61,62].

Conclusion

Based on the results of the study, it can be concluded that, TiO_2NPs alone or in combination with PRP is a promising challenge to promote the acceleration of bone healing and new bone formation.

Financial support and sponsorship

Nil.

Conflicts of interest

None declared.

References

1. Sanz-Martín I, Cha JK, Yoon SW, Sanz-Sánchez I, Jung UW. Long-term assessment of periodontal disease progression after surgical or non-surgical treatment: a systematic review. J Periodontal Implant Sci 2019; 49:60–75.
2. Kattimani V, Lingamaneni KP, Yalamanchili S, Mupparapu M. Use of eggshell-derived nano-hydroxyapatite as novel bone graft substitute – a randomized controlled clinical study. J Biomater Appl 2019; 34:597–614.
3. Sabetrasekh R, Tiainen H, Lyngstadaas SP, Reseland J, Haugen H. A novel ultra-porous titanium dioxide ceramic with excellent biocompatibility. J Biomater Appl 2011; 25:559–580.
4. Löberg J, Perez Holmberg J, Mattisson I, Arvidsson A, Ahlberg E. Electronic properties of nanoparticles films and the effect on apatite-forming ability. Int J Dent 2013; 46:55–60.
5. Falentin-Daudré C, Baumann J-S, Migonney V, Spadavecchia J. Highly crystalline sphere and rod-shaped TiO2 nanoparticles: a facile route to bio-polymer grafting. Arab J Lab Med 2017; 1:217–223.
6. Pilloni A, Pompa G, Saccucci M, Di Carlo G, Rimondini L, Brama M, *et al.* Analysis of human alveolar osteoblast behavior on a nano-hydroxyapatite substrate: an *in vitro* study. BMC Oral Health 2014; 14:1–7.
7. Attia MS, Mohammed HM, Attia MG, Hamid MA, Shoeriabah EA. Histological and histomorphometric evaluation of hydroxyapatite-based biomaterials in surgically created defects around implants in dogs. J Periodontol 2019; 90:281–287.
8. Santos FA, Pochapski MT, Martins MC, Zenóbio EG, Spolidoro LC, Marcantonio JrE. Comparison of biomaterial implants in the dental socket: histological analysis in dogs. Clin Implant Dent Relat Res 2010; 12:18–25.
9. Araújo M, Linder E, Lindhe J. Effect of a xenograft on early bone formation in extraction sockets: an experimental study in dog. Clin Oral Implants Res 2009; 20:1–6.
10. Jafari S, Mahyad B, Hashemzadeh H, Janfaza S, Gholikhani T, Tayebi L. Biomedical applications of TiO2 nanostructures: recent advances. Int J Nanomedicine 2020; 15:3447.
11. Mayer FL, Wilson D, Hube B. Candida albicans pathogenicity mechanisms. Open Dent J 2013; 4:119–128.
12. Civinini R, Macera A, Nistri L, Redl B, Innocenti M. The use of autologous blood-derived growth factors in bone regeneration. Clin Cases Miner Bone Metab 2011; 8:25.
13. Andia I, Abate M. Platelet-rich plasma: underlying biology and clinical correlates. Regen Med 2013; 8:645–658.
14. Alves R, Grimalt R. A review of platelet-rich plasma: history, biology, mechanism of action, and classification. Skin Appendage Disord 2018; 4:18–24.
15. Saleem M, Pisani F, Zahid FM, Georgakopoulos I, Pustina-Krasniqi T, Xhajanka E, *et al.* Adjunctive platelet-rich plasma (PRP) in infrabony regenerative treatment: a systematic review and RCT's meta-analysis. Stem Cells Int. 2018;46:77.
16. Ucuzian AA, Gassman AA, East AT, Greisler HP. Molecular mediators of angiogenesis. J Burn Care Res 2010; 31:158–175.
17. Ferrara N, Gerber H-P, LeCouter J. The biology of VEGF and its receptors. Nat Med 2003; 9:669.
18. Accorsi-Mendonça T, da Silva Paiva KB, Zambuzzi WF, Cestari TM, Lara VS, Sogayar MC, *et al.* Expression of matrix metalloproteinases-2

and-9 and RECK during alveolar bone regeneration in rat. J Mol Histol 2008; 39:201–208.

19. Nguyen M, Arkell J, Jackson CJ. Human endothelial gelatinases and angiogenesis. Int J Biochem Cell Biol 2001; 33:960–970.

20. Liang HPH, Xu J, Xue M, Jackson CJ. Matrix metalloproteinases in bone development and pathology: current knowledge and potential clinical utility. Metalloproteinases Med 2016; 3:93–102.

21. Dhurat R, Sukesh M. Principles and methods of preparation of platelet-rich plasma: a review and author's perspective. J Cutan Aesthet Surg 2014; 7:189.

22. Young S, Bashoura AG, Borden T, Baggett LS, Jansen JA, Wong M, *et al*. Development and characterization of a rabbit alveolar bone nonhealing defect model. Sports Med Arthrosc Rehabil Ther Technol 2008; 86:182–194.

23. J. KGK. *Education guide: special stains and H & E*. Carpinteria, California; Dako North America; 2010.

24. Bratthauer GL. The avidin–biotin complex (ABC) method and other avidin–biotin binding methods. Methods Mol Biol 2010; 588:257–270.

25. Klein M, Vignaud JM, Hennequin V, Toussaint B, Bresler L, Plenat F, *et al*. Increased expression of the vascular endothelial growth factor is a pejorative prognosis marker in papillary thyroid carcinoma. J Clin Endocrinol Metab 2001; 86:656–658.

26. Nemcovsky CE, Nart J. Modern clinical procedures in periodontal reconstructive treatment. Clin Dent Rev 2019; 3:87–123.

27. Bayani M, Torabi S, Shahnaz A, Pourali M. Main properties of nanocrystalline hydroxyapatite as a bone graft material in treatment of periodontal defects. A review of literature. Biotechnol Biotechnol Equip 2017;31:215–220.

28. Wang J, Wang L, Fan Y. Adverse biological effect of TiO2 and hydroxyapatite nanoparticles used in bone repair and replacement. Int J Mol Sci 2016; 17:798.

29. Anitua E. Plasma rich in growth factors: preliminary results of use in the preparation of future sites for implants. Int J Oral Maxillofac Implants 1999; 14:529–535.

30. Martinez-Martinez A, Ruiz-Santiago F, Garcia-Espinosa J. Platelet-rich plasma: myth or reality?. Radiología 2018; 60:465–475.

31. Giannini S, Cielo A, Bonanome L, Rastelli C, Derla C, Corpaci F, *et al*. Comparison between PRP, PRGF and PRF: lights and shadows in three similar but different protocols. Eur Rev Med Pharmacol Sci 2015; 19:927–930.

32. Kothari K. Role of platelet-rich plasma: the current trend and evidence. Indian J Pain 2017; 31:1.

33. Schliephake H. Bone growth factors in maxillofacial skeletal reconstruction. Int J Oral Maxillofac Surg 2002; 31:469–484.

34. Canbeyli İD, Akgun RC, Sahin O, Terzi A, Tuncay İC. Platelet-rich plasma decreases fibroblastic activity and woven bone formation with no significant immunohistochemical effect on long-bone healing: an experimental animal study with radiological outcomes. J Orthop Surg Res 2018; 26:23–66.

35. Marie PJ. Fibroblast growth factor signaling controlling bone formation: an update. Gene 2012; 498:1–4.

36. Smolec O, Radišić B, Liu Z, Kai F, Brkljača Bottegaro N, Pećin M, *et al*. The influence of transforming growth factor beta-1 proven in autologous omental graft on the healing of critical size defects in rabbit radius. Vet Arh 2013; 83:189–199.

37. Marx RE, Carlson ER, Eichstaedt RM, Schimmele SR, Strauss JE, Georgeff KR. Platelet-rich plasma: growth factor enhancement for bone grafts. Oral Surg Oral Med Oral Pathol Oral Radiol Endod 1998; 85:638–646.

38. Plachokova A, Van den Dolder J, Van Den Beucken J, Jansen J. Bone regenerative properties of rat, goat and human platelet-rich plasma. Int J Oral Maxillofac Surg 2009; 38:861–869.

39. Rodriguez IA, Growney Kalaf EA, Bowlin GL, Sell SA. Platelet-rich plasma in bone regeneration: engineering the delivery for improved clinical efficacy. Biomed Res Int 2014; 2014:55–73.

40. Roffi A, Filardo G, Kon E, Marcacci M. Does PRP enhance bone integration with grafts, graft substitutes, or implants? A systematic review. BMC Musculoskelet Disord 2013; 14:330.

41. Döri F, Huszar T, Nikolidakis D, Tihanyi D, Horvath A, Arweiler NB, *et al*. Effect of platelet□rich plasma on the healing of intrabony defects treated with beta tricalcium phosphate and expanded polytetrafluoroethylene membranes. J Periodontol 2008; 79:660–669.

42. Webster TJ, Smith TA. Increased osteoblast function on PLGA composites containing nanophase titania. J Biomed Mater Res A 2005; 74:677–686.

43. Santiago-Medina P, Sundaram P, Diffoot-Carlo N. Titanium oxide: a bioactive factor in osteoblast differentiation. Int J Dent 2015; 45:55–88.

44. Katagiri T, Watabe T. Bone morphogenetic proteins. Cold Spring Harbor Persp Biol 2016; 8:21899.

45. Tiainen H, Wohlfahrt JC, Verket A, Lyngstadaas SP, Haugen HJ. Bone formation in TiO2 bone scaffolds in extraction sockets of minipigs. Acta Biomater 2012; 8:2384–2391.

46. Buzarovska A, Gualandi C, Parrilli A, Scandola M. Effect of TiO2 nanoparticle loading on Poly (L-lactic acid) porous scaffolds fabricated by TIPS. Compos B Eng 2015; 81:189–195.

47. Schmitz JP, Hollinger JO. The critical size defect as an experimental model for craniomandibulofacial nonunions. Clin Orthop Relat Res 1986; 205:299–308.

48. Lu M, Rabie A. Microarchitecture of rabbit mandibular defects grafted with intramembranous or endochondral bone shown by micro-computed tomography. Br J Oral Maxillofac Surg 2003; 41:385–391.

49. Zhang J, Lu H, Lv G, Mo A, Yan Y, Huang C. The repair of critical-size defects with porous hydroxyapatite/polyamide nanocomposite: an experimental study in rabbit mandibles. Int J Oral Maxillofac Surg 2010; 39:469–477.

50. Arafat SW, Kamel SM, Hossam AM, Sabry D. Assesment of bone regeneration of critical size mandibular defects using adipose derived stem cells: an experimental comparative study. Egypt Dent J 2017; 63:2235–2246.

51. Alsousou J, Thompson M, Hulley P, Noble A, Willett K. The biology of platelet-rich plasma and its application in trauma and orthopaedic surgery: a review of the literature. J Bone Joint Surg Am 2009; 91:987–996.

52. Kim ES, Kim JJ, Park EJ. Angiogenic factor-enriched platelet-rich plasma enhances *in vivo* bone formation around alloplastic graft material. J Adv Prosthodont 2010; 2:7–13.

53. Bir SC, Esaki J, Marui A, Yamahara K, Tsubota H, Ikeda T, *et al*. Angiogenic properties of sustained release platelet-rich plasma: characterization in-vitro and in the ischemic hind limb of the mouse. J Vasc Surg 2009; 50:870–879.

54. Honnegowda TM, Kumar P, Udupa E, Kumar S, Kumar U, Rao P. Role of angiogenesis and angiogenic factors in acute and chronic wound healing. Plast Aesthet Res 2015; 2:243–249.

55. Kumar I, Staton C, Cross S, Reed M, Brown N. Angiogenesis, vascular endothelial growth factor and its receptors in human surgical wounds. Br J Surg 2009; 96:1484–1491.

56. Boëck-Neto R, Artese L, Piattelli A, Shibli J, Perrotti V, Piccirilli M, *et al*. VEGF and MVD expression in sinus augmentation with autologous bone and several graft materials. Oral Dis 2009; 15:148–154.

57. Di Stefano DA, Artese L, Iezzi G, Piattelli A, Pagnutti S, Piccirilli M, *et al*. Alveolar ridge regeneration with equine spongy bone: a clinical, histological, and immunohistochemical case series. Clin Implant Dent Relat Res 2009; 11:90–100.

58. Lynch M, Bashir S. Applications of platelet-rich plasma in dermatology: a critical appraisal of the literature. J Dermatolog Treat 2016; 27:285–289.

59. Fitzpatrick J, Bulsara M, Zheng MH. The effectiveness of platelet-rich plasma in the treatment of tendinopathy: a meta-analysis of randomized controlled clinical trials. Am J Sports Med 2017; 45:226–233.

60. Lacci KM, Dardik A. Platelet-rich plasma: support for its use in wound healing. Yale J Biol Med 2010; 83:1.

61. Shin HS, Oh HY. The effect of platelet-rich plasma on wounds of OLETF rats using expression of matrix metalloproteinase-2 and-9 mRNA. Arch Plast Surg 2012; 39:106.

62. Ribeiro A, Gemini-Piperni S, Travassos R, Lemgruber L, Silva R, Rossi A, *et al*. Trojan-like internalization of anatase titanium dioxide nanoparticles by human osteoblast cells. Sci Rep 2016; 6:1–11.